



This is a repository copy of *Upward flame spread behaviour of cladding materials on a medium-scale ventilated façade experimental setup with a single combustible wall*.

White Rose Research Online URL for this paper:

<https://eprints.whiterose.ac.uk/206188/>

Version: Published Version

---

**Article:**

Mendez, J.E. [orcid.org/0000-0001-5552-9030](https://orcid.org/0000-0001-5552-9030), McLaggan, M.S. [orcid.org/0000-0002-4173-5615](https://orcid.org/0000-0002-4173-5615) and Lange, D. (2024) Upward flame spread behaviour of cladding materials on a medium-scale ventilated façade experimental setup with a single combustible wall. *Fire Safety Journal*, 142. 104020. ISSN 0379-7112

<https://doi.org/10.1016/j.firesaf.2023.104020>

---

**Reuse**

This article is distributed under the terms of the Creative Commons Attribution (CC BY) licence. This licence allows you to distribute, remix, tweak, and build upon the work, even commercially, as long as you credit the authors for the original work. More information and the full terms of the licence here:

<https://creativecommons.org/licenses/>

**Takedown**

If you consider content in White Rose Research Online to be in breach of UK law, please notify us by emailing [eprints@whiterose.ac.uk](mailto:eprints@whiterose.ac.uk) including the URL of the record and the reason for the withdrawal request.



[eprints@whiterose.ac.uk](mailto:eprints@whiterose.ac.uk)  
<https://eprints.whiterose.ac.uk/>



# Upward flame spread behaviour of cladding materials on a medium-scale ventilated façade experimental setup with a single combustible wall

Julian E. Mendez<sup>a,\*</sup>, Martyn S. McLaggan<sup>b</sup>, David Lange<sup>a</sup>

<sup>a</sup> The University of Queensland, Brisbane St Lucia, QLD, 4072, Australia

<sup>b</sup> University of Sheffield, Sheffield, S1 3JD, UK

## ARTICLE INFO

### Keywords:

Cladding  
Façade fire  
Flame spread  
Fire growth  
Heat release rate  
Heat transfer  
Ignition

## ABSTRACT

A parametric experimental study was performed to characterise the fire spread dynamics in a simplified ventilated façade using a medium-scale testing rig comprised of a non-combustible and a combustible cladding wall (1800 × 600 mm). Three different cavity widths and four different cladding materials were tested. Measurements of the flame height, the incident heat flux on the non-combustible cavity wall and oxygen consumption calorimetry were performed. A strong relationship between flame height and heat release rate was found for the growth phase of the fire. It has been shown that the time for encapsulation failure and subsequent cladding material core ignition decreased as the cavity width was reduced since the heat transfer to the walls was enhanced. The increase in the heat transfer to the opposite wall with all the materials could lead to external heat fluxes above the critical heat flux for ignition of a number of combustible cladding materials. This highlights the importance of considering the interaction of the products used in the façade and its geometry for the design of façade assemblies when accounting for the fire performance of the system. The results also show the need to understand the impact of the interaction between the design variables and the system performance, since the material performance observed at bench-scale may fail to capture the performance in heat transfer and flame spread scenarios observed at a system scale.

## 1. Introduction

### 1.1. Background

Contemporary building envelopes are a practical way to lower energy consumption. Modern façades however have been shown to have performance in fire which is difficult to predict and their installation has often disregarded their impact of fire spread via the external building envelope on a building's fire safety strategy. This has led to an increase in the number of high-rise building fires with unacceptable fire safety outcomes [1]. The Shanghai fire, which claimed 58 lives [2], and the Grenfell Tower fire, which claimed 72 lives [3], stand out among these fires.

The spread of fire from one floor to another has the potential to compromise a building's fire safety strategy if the consequences of this scenario are not adequately addressed. Whilst there are numerous mechanisms by which vertical fire spread can occur, in the two examples given in the previous paragraph the façade played a critical role in this. Therefore, determining the ability of fire to propagate via a building's

façade system and quantifying the potential fire spread rates become necessary to ensure that a fire safety strategy is able to meet the fundamental objectives of fire safety design [4]. Numerous efforts have been made to quantify the potential fire spread rate in facade systems. However, upward flame spread within a facade assembly often features multiple competing and interacting phenomena such as heat transfer mechanisms, thermal decomposition and thermomechanical effects, as discussed by Torero (see Fig. 1 a) [5]. It is still unknown how to address these complicated systems in order to provide a quantitative performance assessment that enables fire safety engineers to clearly define an effective fire safety strategy.

### 1.2. Upward flame spread in parallel walls

Flame spread is a fundamental problem in fire research, and its characterisation has practical value in fire safety. For flame to propagate on a solid surface, sufficient heat must be transferred from the burning region to the unburned solid to heat and pyrolyze a length of unburnt fuel. Rate of heat transfer and the length over which it occurs heavily

\* Corresponding author.

E-mail address: [j.mendez@uq.edu.au](mailto:j.mendez@uq.edu.au) (J.E. Mendez).

<https://doi.org/10.1016/j.firesaf.2023.104020>

Received 10 June 2023; Received in revised form 3 October 2023; Accepted 5 October 2023

Available online 10 October 2023

0379-7112/© 2023 The Authors. Published by Elsevier Ltd. This is an open access article under the CC BY license (<http://creativecommons.org/licenses/by/4.0/>).

influences the flame spread rate over the fuel. Extensive research regarding the controlling mechanisms of flame spread is available in the literature [7–11].

Upward flame spread over a solid fuel is a specific case of a concurrent flame spread problem, where the buoyancy-induced flows are driven upward. When occurring on a single vertically configured surface, upward flame spread is considered a self-accelerating process. Once a second surface is included this is considered as flame spread within a cavity. The upward flame spread in these scenarios is influenced by a number of factors including the properties of the fuel, the ventilation and geometry of the cavity, and the presence of any fire retardants.

1.2.1. Effect of cavity width

One of the key factors that affects upward flame spread in cavities is ventilation. Adequate ventilation can provide oxygen necessary to support the combustion process and enhance chimney effects (See Fig. 1 (b)), while insufficient ventilation can lead to a decrease in the flame spread rate, even leading to quenching of the flame for cavities with small enough separation. Several studies have been conducted relating the effect of the separation of parallel surfaces on the flame spread over combustible materials. Shi and Wu conducted an experimental study to characterise the upward flame spread over solid fuels and the effect of interactions between multiple surfaces. The authors found that the flame spread rate exhibits a non-monotonic behaviour in respect to the separation of the walls. This is because: 1) the convective and radiative thermal exchange between flames and solids increases the forward heat transfer rates to the solids, and the interactions become stronger as the separation distance is reduced; however, 2) when the separation between the walls is very small, the flames present in the cavity have restricted thermal expansion in limited space and a shortage of oxygen availability which leads to a lower rate of spread if compared with intermediate separation distances [12]. It has elsewhere been observed that the presence of a second wall enhances the thermal heat transfer to the solids [13–15] and hence flame spread rate is faster for the parallel wall configuration than that for a single fuel [12]. Zhao et al. developed an experimental study on the effects of including an opposed vertical wall on upward flame spread over polymethyl methacrylate (PMMA). It was observed that the flame height first increases and then decreases with an increase in the gap between the curtain walls, before reaching a constant value [16].

Some studies have considered flame spread on façade assemblies comprising a number of cladding materials. Ma et al. conducted an experimental study on interlayer effect induced by a curtain wall on the burning behaviour of a flexible polyurethane insulation foam (800 mm

long, 200 mm wide, 20 mm thick). The study found that average flame height first increased and then decreased as the distance between the insulation foam and the curtain wall increased. A critical distance for the largest flame height was found at a separation of 0.10 m [17]. An et al. investigated the effects of a parallel curtain wall on downward flame spread on insulation materials (600 mm long, 100 mm wide, 40 mm thick) used in façades. It was found that the flame height has a non-monotonic distribution with wall separation. The authors concluded that the total heat feedback from the curtain wall to the façade material decreases exponentially with the decrease of separation and that the radiant feedback is the dominant heat transfer mechanism compared with convective heat transfer [18]. Although these studies present interesting findings on the mechanisms of flame spread on insulation foam materials, the sample size is reduced to thin slabs of pure material, which disregards possible edge effects and the role of the encapsulation layer on fire spread. Additional research was conducted at the University of Edinburgh to investigate the fire spread in Grenfell Tower [19] and the flammability of the materials used in the tower [20], specifically the aluminium composite panels (ACPs) and insulation products. This research demonstrated that there is an extreme complexity in the growth of fires in ventilated facades incorporating combustible cladding or insulation products. This study concluded that the factor most likely to drive the fire growth and spread over the ACP is whether the opposing wall provides heat to the region far away from the ignition leading to a self-sustaining fire growth regardless of the combustibility of the opposing wall [19]. The work also evaluated the effect of encapsulation on the insulation foam and investigated the key phenomena leading to sustained fire growth in a cavity with combustible materials for both walls. The study however was not intended to be generalised, was focused on a very specific setup and concerned the ignition and burning of the ACP PE and the factors affecting this, including the presence of the cavity, the effect of the insulation properties, and the presence of encapsulation on the insulation foam.

1.2.2. Effect of material properties

The flammability properties of the fuel also have a significant impact on the flame spread rate in modern facades. McLaggan et al. [21] presented common trends in the ignition and burning behaviour for cladding materials in a systematic bench-scale study using the Cladding Material Library [22]. The authors highlighted that organic content is a poor indicator of the fire performance and that a proper assessment of the flame spread in bench-scale tests needs to be conducted. McLaggan et al. [23] found the ratio of time to ignition and the time to burnout ( $t_{ig}/t_{bo}$ ) and the preheated flame length ( $L_{ph}$ ) as the critical limiting conditions for evaluating flame spread which can ultimately be

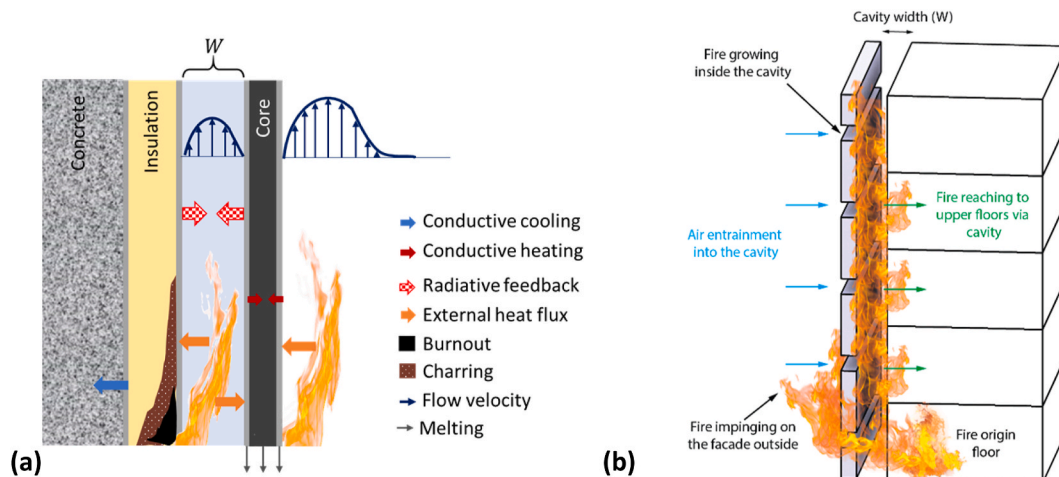


Fig. 1. (a) Physical phenomena in upward flame spread in a cavity (adapted from Ref. [5]). (b) Flame spread in a façade (adapted from Ref. [6]).

evaluated at the material-level, through an analysis of the flame spread velocity equations. Torero [24] presents a thorough review and detailed analysis and similarly presents the importance of  $L_{ph}$ . Other relevant material and bench scale flammability properties for the prediction of flame spread include but are not limited to thermal inertia, ignition temperature, and heat released by the material. Another important factor that affects upward flame spread is the presence of any fire-retardant materials which are able to suppress the flame and prevent heat feedback to the material.

1.3. Research significance

The aforementioned effect of different variables and phenomena needs to be decoupled in order to reach a better understanding of the fire dynamics, based on a gradual increasing in complexity of the system studied. The authors previously presented a study of fire dynamics in ventilated cavities with non-combustible linings [13], which highlighted the impact of reducing the cavity width on heat transfer and the potential of this design variable to accelerate the ignition and flame spread over combustible materials. This paper presents a parametric experimental study that characterises the effect of cavity width and material flammability on the upward flame spread on the same setup but with one surface replaced with combustible cladding materials, as well as the heat transfer to the non-combustible lining. This removes the complexity of two materials burning simultaneously in a typical ventilated façade assembly as has partly been explored by Bisby [19], but still generates useful data on a single burning surface within a cavity setup. The findings of this paper will contribute to an improved understanding on the effect of this variables on the upward flame spread on a façade assembly.

2. Material and methods

2.1. Experimental setup description – dimensions and lining properties

The experimental setup consisted of two 600 mm wide, 1800 mm high walls placed in a parallel configuration and mounted on an aluminium frame (see Fig. 2(a),b)). One of the walls was made of vermiculite and is referred as the “non-combustible wall”. The thermal properties for this material are presented as supplementary data in Table S1 and are provided by the manufacturer [25]. The combustible linings were installed in the opposite wall featuring one of two types of Aluminium Composite Panels (ACPs) or one of two types of Insulation foam (INS). This opposite wall was mounted over movable elements that

allowed to slide the support element to provide the desired cavity width. The cavity widths were chosen to match the values in a previous study [13]. The thermal properties of the combustible linings were determined using the Detailed Testing Protocol from the Cladding Material Library (CML) [26] and are presented in Table 1.

All of the tested cladding materials were covered by encapsulating elements. Combustible insulation foams featured a foil front, while ACPs featured a polymeric core covered by a metallic encapsulation (aluminium). The role of this encapsulation element is crucial to the fire growth in each of these cladding systems. The encapsulation may prevent or slow the pyrolysis gases from combining with air and igniting, which delays the ignition of the polymeric cores. Besides the thermal

Table 1  
Cladding materials properties.

Material	ACP-FR	ACP-PE	PIR	PF
Description (CLM key name)	ACP with a core consisting of polyethylene and a fire retardant	ACP with a core consisting of polyethylene	Polyurethane-based polyisocyanurate foam (INS01)	Phenolic foam (INS02)
Gross heat of combustion (kJ/g)	20.14	38.98	30.0	26.5
Apparent thermal inertia ( $kW^2s.K^{-2}.m^{-4}$ )	1.122	1.273	0.037	0.080
Ignition temperature ( $^{\circ}C$ )	423	321	458	417
Critical heat flux for ignition ( $kW.m^{-2}$ )	19.5	11.5	23.0	18.9
Heat flux range ( $kW.m^{-2}$ )	35–60	35–60	35–60	35–60
Peak heat release rate per unit area ( $kW.m^{-2}$ )	131–175	397–615	150–223	62–89
Core thickness (mm)	3	3	80	80
Encapsulation thickness (mm)	0.5	0.5	0.01	0.01

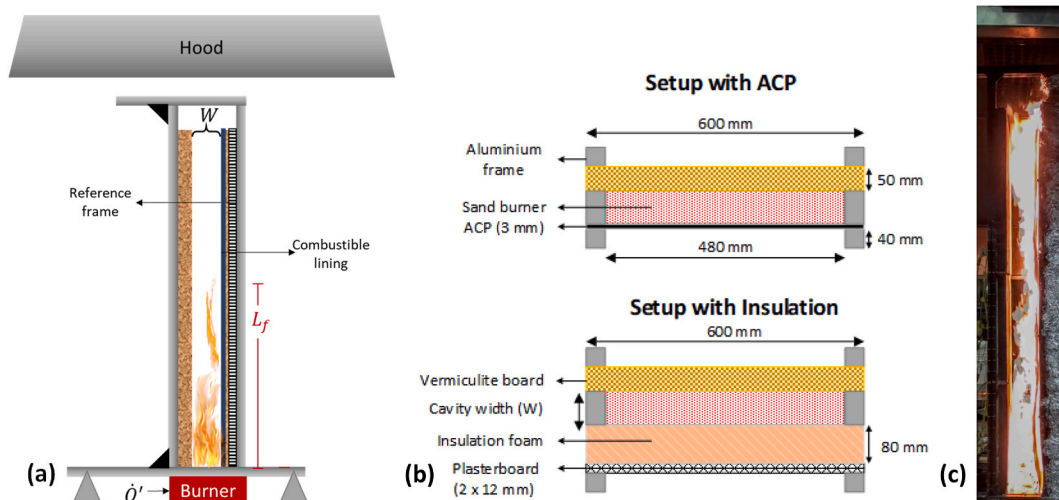


Fig. 2. Experimental setup components (a)Schematic Lateral view. (b)Schematic plan view with ACP (top), and insulation foam (bottom). (c)Lateral view.

properties of the materials, the encapsulation has an effect on the heat transfer, since the decreased emissivity of the foil facing elements means that they reflect a small portion of the radiation from the flame or a heated opposite wall. Once the encapsulation is compromised a fast fire growth and spread is observed.

## 2.2. Burner

A sand methane burner was placed at the base of the parallel walls to serve as source of fire. The heat release rate was fixed at 16.8 kW (corresponding to a HRR per unit length of the burner of 35 kW/m). The heat release rate was controlled using a Teledyne HFC-D-303B mass flow controller. The length of the burner was kept constant at 480 mm. This parameter was set to be shorter than the wall width to avoid having flames escaping the cavity in the early stages of the fire, i.e. before any ignition of the combustible linings. The width of the burner was modified to match the width of the cavity by having an aperture at the top of the burner which had the fixed length and width corresponding to the cavity wall. This configuration was also set with the intent to use previously obtained data that corresponds to a semi steady state where the flame of the burner was constrained between two non-combustible parallel walls [27]. The experimental configurations which were investigated are presented in Table 2.

Three different cavity widths were used for each cladding material by mounting the non-combustible wall over movable elements that allowed to provide the desired cavity width. Tests were run for 90 min, unless the fuel was completely consumed and HRR returned to 0, in which case the test was stopped after a further period of 5 min. In one case, marked with an asterisk, the test was stopped early because smoke escaped the hood and represented a safety hazard in the lab. Nonetheless, results in this paper focus on the fire growth phase, and the termination of the test therefore has no impact on the analysis.

Every test was carried out twice. The intent of the setup is to reach a better understanding of the effect of the variation of the cavity width and material properties on the flame spread velocity and burning rate. The experimental setup was placed under an extraction hood in order to measure the heat release rate of the fire. The HRR from the burner is subtracted from the total HRR in the results presented below. The HRR was determined using Oxygen Consumption calorimetry. All the tests were recorded on video in order to extract the flame height of the fire generated by the burner.

## 2.3. Flame height and flame spread velocity determination

Flame heights were measured as the tip of the continuous flame from an individual frame per second, extracted from a video taken during the tests (see Fig. 2 c)) during the duration of the test. A reference frame was included into the experimental setup to calibrate the height and to account for visual effects due to perspective. The flame height profile was smoothed and converted into flame spread velocity by using Eq. 1

**Table 2**

Experimental campaign conditions. Two repetitions (R1/R2) were carried for each configuration.

Test	Cavity width (W) [m]	Material
ACP FR-W050-R1/R2	0.05	ACP-FR
ACP PE-W050-R1/R2*	0.05	ACP-PE
ACP FR-W100-R1/R2	0.10	ACP-FR
ACP PE-W100-R1/R2	0.10	ACP-PE
ACP FR-W150-R1/R2	0.15	ACP-FR
ACP PE-W150-R1/R2	0.15	ACP-FR
PIR-W050-R1/R2	0.05	PIR
PF-W050-R1/R2	0.05	PF
PIR-W100-R1/R2	0.10	PIR
PF-W100-R1/R2	0.10	PF
PIR-W150-R1/R2	0.15	PIR
PF-W150-R1/R2	0.15	PF

$$V_s = \Delta L_f / \Delta t \quad (1)$$

The data for the flame spread velocity is presented for a subset of the experiments in the supplementary data.

## 2.4. Heat flux calculation and measurement

The non-combustible wall was equipped with thin-skin calorimeters (TSCs) to calculate the total external heat flux, and 1.5 mm type-K thermocouples in order to measure the gas-phase and solid-phase temperatures. The specifications for the TSCs are described in more detail by Mendez et al. [13]. Fig. 3 (a) shows the location of the temperature sensors. The heat flux impinging the ancillary wall arises because of the heat provided by the flame of the burner and the combustion of the combustible lining. The TSCs were then grouped on different regions to characterise the spread of the flames along the combustible lining as indicated in Fig. 3 (d).

The total external heat flux on the wall was defined as the sum of a radiative and a convective component.

$$\dot{q}_T = \dot{q}_r + \dot{q}_c \quad (2)$$

The radiative component was calculated using the methodology proposed by Hidalgo. et al. [28], as described by Eq. (3).

$$\dot{q}_r(T_s) = \frac{1}{\alpha_{TSC}(1-C)} \left[ \rho \delta C_P \frac{dT}{dt} + \epsilon_{TSC} \sigma (T_s^4 - T_{gas}^4) + h_c (T_s - T_\infty) \right] \quad (3)$$

where  $\alpha_{TSC}$  is the absorptivity of the TSC metal disc,  $C$  is a correction factor for the heat transfer by conduction,  $\rho_{TSC}$  is the density of the TSC metal disc,  $\delta_{TSC}$  is the thickness of the disc,  $C_{P,TSC}$  is the specific heat capacity of the disc,  $\epsilon_{TSC}$  is the emissivity of the disc,  $\sigma$  is the Stefan-Boltzmann constant,  $T_s$  is the solid-phase temperature measured by the TSC and  $T_\infty$  is the environment temperature. While the convective component was defined as:

$$\dot{q}_c = h_c (T_{gas} - T_\infty) \quad (4)$$

The validation of the Thin Skin Calorimeters (TSCs) is out of the scope of this study since these have already been validated previously [28] and used elsewhere as reported in the literature [13,29]. Additionally, the wall comprised of the cladding material was instrumented with 5 in-depth thermocouples positioned in the centreline of wall, beneath the encapsulation layer facing the fire, in order to measure the in-depth temperature for the combustible material at heights of 100, 500, 900, 1300 and 1700 mm. A discussion of this data is not included in this manuscript since this does not add value for or against the conclusions already drawn using the other instrumentation.

## 2.5. Estimation of experimental errors

A summary of the sources of uncertainty linked to experimental error are presented in Table 3. The total expanded uncertainty is calculated as the sum of the root-sum square of the systematic uncertainties ( $B_i = RSS(B_i)$ ) and the Root-sum square random uncertainties ( $S_i = RSS(S_i)$ ), corrected by a factor of 2, to account for a 95 % confidence interval (2 standard deviations) as defined by the ASME/ANSI Performance Test Code [30], as per Eq. (5).

$$U_t = 2 \left( \left( \frac{B_t}{2} \right)^2 + (S_t)^2 \right)^{0.5} = 2C_t \quad (5)$$

The uncertainties for the instruments were determined based on statistical methods, specifications of the instrument, calibration reports and random uncertainties. Thermocouples had a calibration uncertainty of  $\pm 1.5$  °C or  $\pm 0.55$  % of the measurement reading. The error due to radiation was deemed to be between 0 % to -6 % according to available literature [31]. TSCs had a calibration uncertainty of  $\pm 3$  %, and

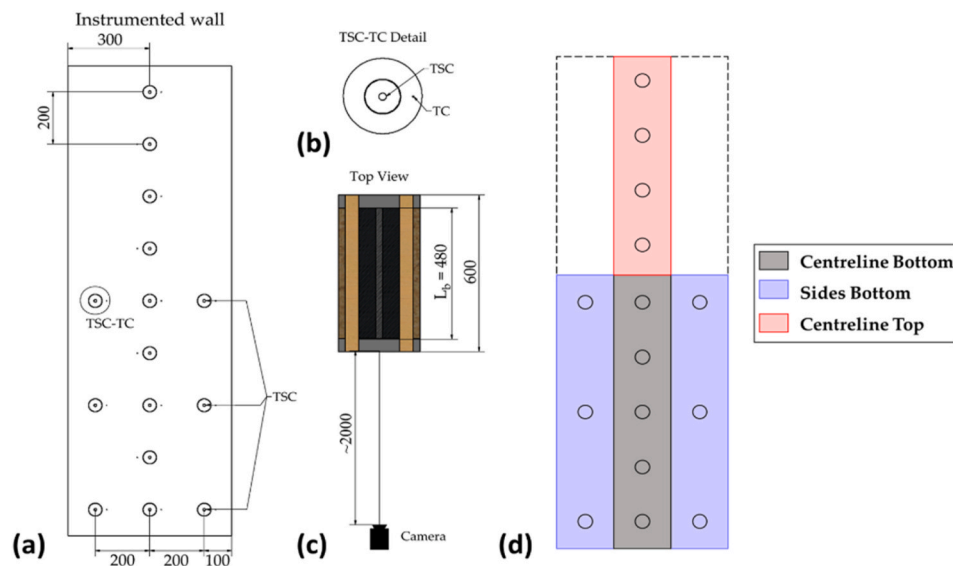


Fig. 3. a) Location of the thermal sensors on the vermiculite wall. b) Detailed location of TSCs and TCs. c) Camera location - plan view. d) Groups of thermal sensors.

Table 3  
Measurement of experimental uncertainty.

Sensor	Uncertainty source	Type of uncertainty	Uncertainty ( $S_i$ or $B_i$ )	Combined Standard Uncertainty ( $C_i$ )	Total expanded uncertainty ( $U_i$ )
Thermocouple	Calibration	B	$\pm 0.55\%$	-5.2 to 3.0 %	-10.4 to 6.1 %
	Radiation	B	-6.0 to 0 %		
	Random	S	$\pm 3.0\%$		
TSCs	Calibration	B	$\pm 3.0\%$	4.9 %	9.7 %
	Radiative heat balance	B	$\pm 4.5\%$		
	Random	S	$\pm 3.0\%$		
Gas Analyser	Zero and span gas calibration	B	$\pm 1.0\%$	5.9 %	11.7 %
	Equipment uncertainty	B	$\pm 1.0\%$		
	Mixing and averaging	B	$\pm 7.0\%$		
	Random	S	$\pm 3.0\%$		

uncertainty related to the radiative heat transfer balance of  $\pm 4.5\%$ , as determined in previous studies [13,28]. The uncertainties associated with the calorimetry can be related to the calibration of the zero and span gases ( $\pm 1\%$ ) and averaging errors due to the sampling lines ( $\pm 7\%$ ). An additional random uncertainty of  $\pm 3\%$  was added for all the measurement devices, as indicated by per previous studies on experimental uncertainty [31,32].

The obtained values for the combined standard uncertainty and total expanded uncertainty are in line with values for experimental studies

available in the literature [31–33].

### 3. Results

The results and discussions presented in this work are mainly focused on identifying general trends regarding the contributions of both cladding materials and cavity size to the overall fire growth.

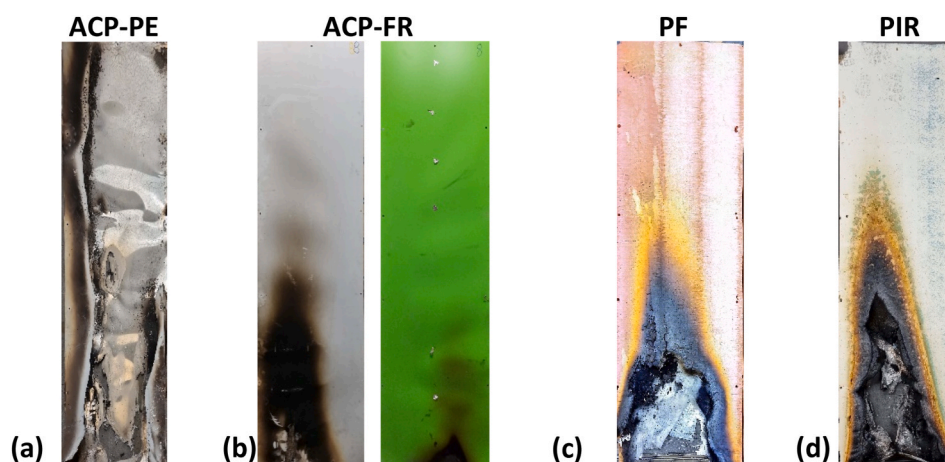


Fig. 4. Cladding materials after test completion.

### 3.1. Material behaviour

The fire growth was heavily dependent on the thermal degradation of the different cladding products. Footage of the aftermath of the experiments is used to describe the behaviour of the samples and its relationship with fire growth. Fig. 4 shows the cladding materials after the test was completed.

The thermal degradation of the ACPs used in this study were considerably different both in regards of the failure of the encapsulation and the subsequent fire spread over the polymeric core. Even if melting of the encapsulation was observed for both products it led to two different subsequent behaviours, as shown in Fig. 4 (a) and (b).

**ACP-PE:** ACP-PE presented a rapid upward fire spread that generated melting of both the polymeric core and the encapsulation layer facing the cavity even reaching the melting of the external encapsulation layer (See Fig. 4(a)).

**ACP-FR:** The failure of the ACP-FR encapsulation was limited and a discolouration of the pigments of the encapsulation was noticed. No sustained flaming of the polymeric core was observed and the residue of the combustion made evident the action of the fire-retardant agent as depicted in Fig. 4(b).

**PF:** Popping noises were noticed at early stages of the test, even before the encapsulation foil was breached. Those noises have been previously observed by Hidalgo et al. [34] and are believed to be caused by spalling, as well as by Scudamore when testing these type of foams in the cone [35]. Additional to the aforementioned sounds, the authors observed foam fragments being ejected from the surface, as previously observed by Scudamore [35]. PF has been shown to char and oxidise severely. This oxidation profile can be seen in Fig. 4 (c). This insulation foam may also ignite quickly when exposed to heat flux values higher than the critical, due to its low thermal inertia. The encapsulation prevents this process from happening, but once this protected layer is breached and detaches from the PF, the insulation foam is charred and oxidised. At low heat flux values PF forms a char layer. If this layer reached a critical depth, the unburnt fuel did not receive enough heat to produce sufficient pyrolysis gases, which led to extinguishment.

**PIR:** The aluminium foil encapsulation laminated to both faces of the foam reduced the heat transfer by radiation, delaying the processes of oxidation and pyrolysis. Fig. 4 (d) shows the PIR foam after the testing concluded and the aluminium foil was peeled off. The portion of the foam where the encapsulation did not fail preserved its original yellow colour, whereas the regions where the encapsulation was breached suffered discolouration has three different distinct with an oxidised orange-brown layer finally followed by a black char layer. As with the

other insulation foam it is believed that once a critical char layer depth was reached, the energy provided by the burner was not enough to sustain the combustion and the flame spread stopped.

### 3.2. Fire growth

The heat release rate for all the combustible linings installed 0.1 and 0.15 m apart from the non-combustible wall are depicted in Fig. 5. All times are measured from the time the gas burner was ignited.

The fire from the burner did not considerably spread across most of the linings for the 150 mm gap configuration, with the exception of the ACP-PE (see Fig. 5, left). It can be observed that for the FR ACP and both insulation foams, the HRR remained almost constant for the duration of the experiment. For the tests with ACP-PE, once the aluminium encapsulation failed (at 9 and 17 min for repetitions 1 and 2 respectively), the fire rapidly spread along the polyethylene core. This led to the largest peak HRR among all the components for this cavity width, around 200 kW.

These results are consistent with the values corresponding to the peak HRR in the material scale, which can be used as an indicator of the fire performance of the façade assembly. The relative magnitude of each material is consistent with those tests conducted for the Grenfell tower enquiry by Bisby with two combustible walls [19]. However, the performance of the assembly and the products that comprise it can also be influenced by other variables such as the cavity width.

Reducing the cavity width to 0.10 m had an effect on the fire growth, where the fire spread along both insulation foams and the ACP-PE. For this cavity width, spread was observed for the insulation foams less than 10 s after the burner ignition, but the flame exclusively spread through the encapsulation layers flickering and quenching once the encapsulation layer charred. A faster failure of the foil encapsulation was observed than for the aluminium in the ACPs. A second growth phase involving the PIR core was observed between 4 and 10 min after the start of the experiment, whereas a second growth phase was observed for the PF foams after 20 min. The time for failure of the ACP-PE encapsulation was significantly reduced to approximately 4 min after the ignition of the burner. This can be explained from the increase on the radiative heat flux impinging the combustible lining with a reduced separation between the walls. This increase in the radiative heat flux is the result of the exposure of the walls to the flames (from the burner and the combustible lining) in a reduced cavity, as previously demonstrated in the literature [13–15]. Additionally, this increase in the radiative heat flux along the surface of the combustible linings can explain the ignition of the foam cores and the moderate spread along the surface of the

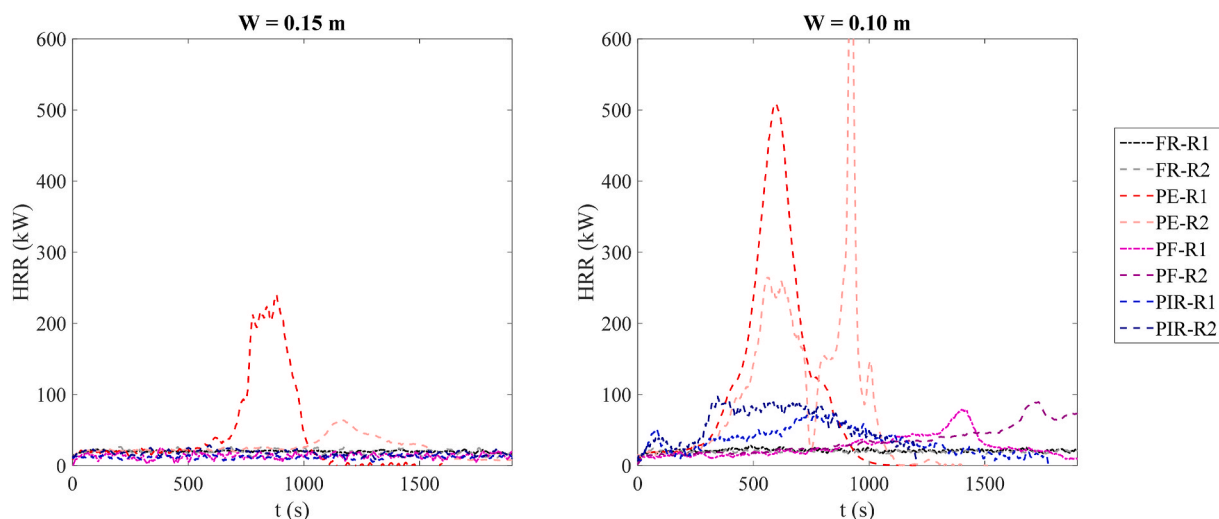


Fig. 5. Heat Release Rate for the different linings.

cladding materials.

The fire growth was also characterised in terms of the flame height. Figs. 6 and 7 present both flame height and HRR as a function of time for a subset of the experiments. A good level of agreement can be observed between both profiles, showing a positive correlation between HRR and flame height, i.e. an increase in heat release rate corresponds with an increase in flame height. This is especially true for the experiments where considerable flame spread was observed (see Fig. 6 (e)-6 (h)).

In the cases where a variation of the flame height was observed, despite the presence of a semi steady HRR value (PIR,  $W = 0.150$  m, (see Fig. 6 (c)–(d))), this variation can be attributed to the spread of the flame through the encapsulation layer but not through the insulation core. The “plateau” values for the flame height for the PIR assemblies with a cavity width of 0.10 m correspond to a limitation of the visualization of the camera and not to a stagnant flame, the flame reached the top of the setup even extending into the extraction hood and these plateau data should not be used to develop correlations between the total HRR and the flame height.

As for the behaviour of the flame in the systems featuring ACPs (see Fig. 7), a semi-steady flame height was observed for the systems with ACP-FR whereas an increase in this variable was observed for ACP-PE core. This aligns with the behaviour obtained at the material scale, considering that due to its heat release rate per unit area, it is expected that the ACP-PE core releases more heat. Flame height is larger since it is proportional to the heat release rate, as more heat being released results in more buoyant upward flow of hot gases and air. A higher HRR leads to an increase in the production of hot gases, which creates a higher buoyant force, resulting in a taller flame, which preheats a larger area leading to a faster rate of pyrolysis.

These observations agree with others in the literature [19] where a larger HRR within the cavity was linked with a more uniform heating of the inside surface of the ACP. This uniform heating led to the inside aluminium encapsulation of the ACP becoming compromised earlier and exposing a larger surface area of PE to burning, enhancing the fire growth. This additional HRR could be provided either by the ACP itself or the combustion of a component fixed at the opposite wall.

Once the flame height was characterised it was of special interest to explore the effect of the heat released by the materials on the opposite wall. The flame spread was then characterised via the heat transfer to the opposite wall.

### 3.3. Effect of flame spread over the cladding materials on the heat transferred to the cavity walls

Figs. 8 and 9 present the evolution of the total external heat flux on the vermiculite wall considering the mapping regions defined in Fig. 3 d). A sudden increase in the heat flux implies the increase of energy received to the opposite wall by either or both convective and radiative heat transfer mechanisms. The first peak displayed in all the test corresponds to the ignition of the burner which leads to a significant increase on the convective heat transfer from the hot combustion gases ascending through the cavity. Once the walls reach a thermal equilibrium there is a temporary decrease in the total external heat flux followed by one of the possible scenarios.

- a) Sudden increase due to the combustion of the cladding material, that leads to the generation of a flame that heats up the instrumented wall
- b) Steady increase of the heat flux due to the progressive heating up of the wall and the thermal feedback between the walls.

Fig. 8 shows the behaviour of the total external heat flux in the systems featuring ACPs. It can be seen that no sustained combustion of the ACP-FR core was observed. Additionally, no flame spread was registered to the upper region of the setup for the two larger cavities, since no considerable increase of the external heat flux was observed for this region. That is not the case for the narrowest cavity, where the upper centreline region registers similar values to the bottom region. This is because as the cavity width is reduced, the radiative feedback between the walls increases, as well as the convective and radiative thermal exchange between flames and solids, which enhances the heat transfer rates to the walls of the cavity. The potential interaction among different combustible materials is out of the scope of this research but it could shed light on the upward flame spread in an external façade assembly.

As for the ACP-PE, flame spread within the lining can be noticed from the sudden rise in the external heat flux for all the cavities. A lower total external heat flux can be noticed at the upper region for the largest cavity width which implies lower heat transfer from either the combustion of the ACP-PE panel or the increase of the radiative feedback to the opposite wall. For the 0.10 and 0.15 m cavities, the external heat flux on the walls surpasses 100 kW/m<sup>2</sup> which could lead to the potential thermal decomposition of the encapsulation and ignition of the core of most cladding materials. As for the narrowest cavity (50 mm), the total heat transferred to the opposite wall was reduced since both the internal

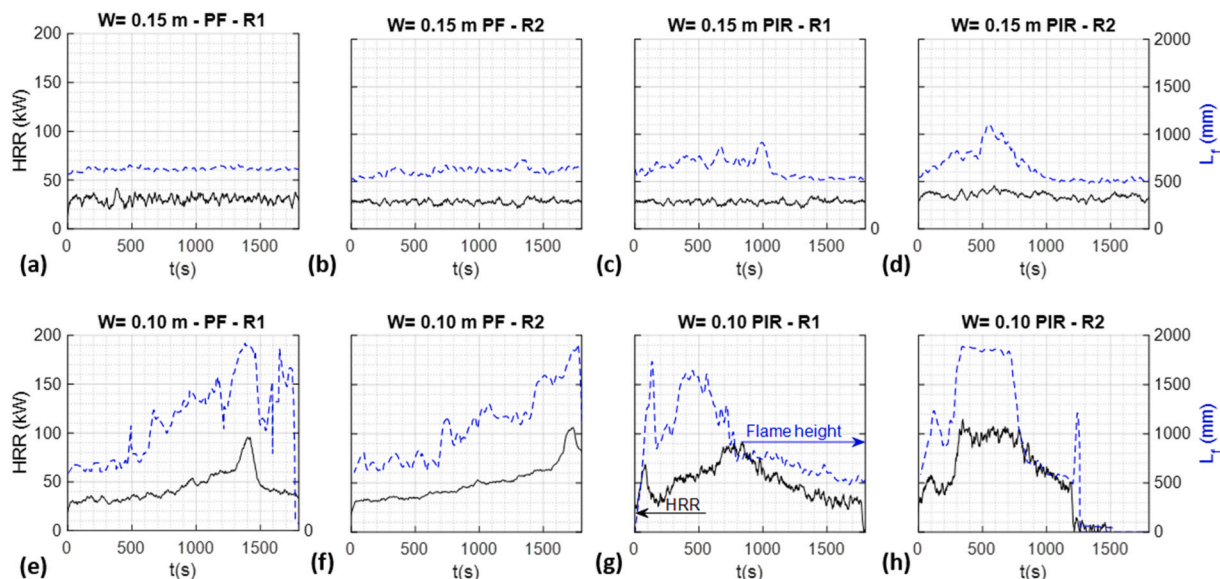


Fig. 6. Transient flame height (blue dashed lines) and HRR (black line) for the insulation foams

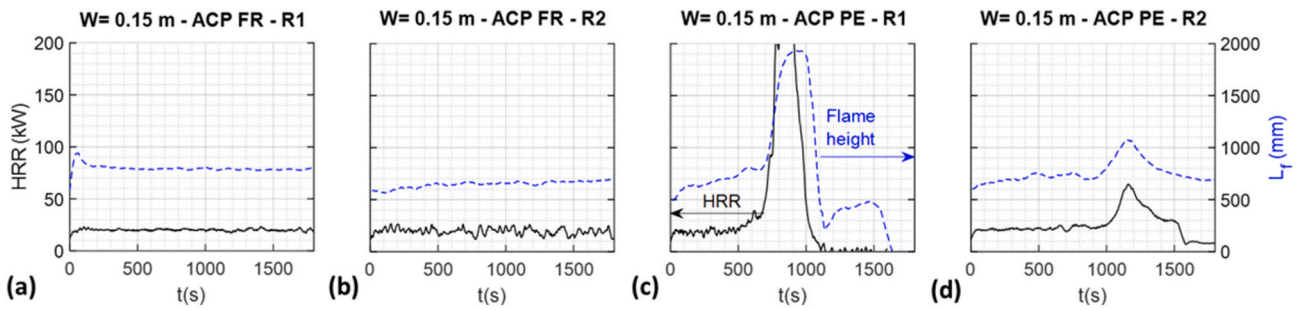


Fig. 7. Transient flame height (blue dashed lines) and HRR (black line) for the ACPs. Note that when the flame exceeds the height of the setup, the exact measurement of peak HRR is not particularly relevant and so the plot is instead capped at 200 kW to clarify the rest of the data.

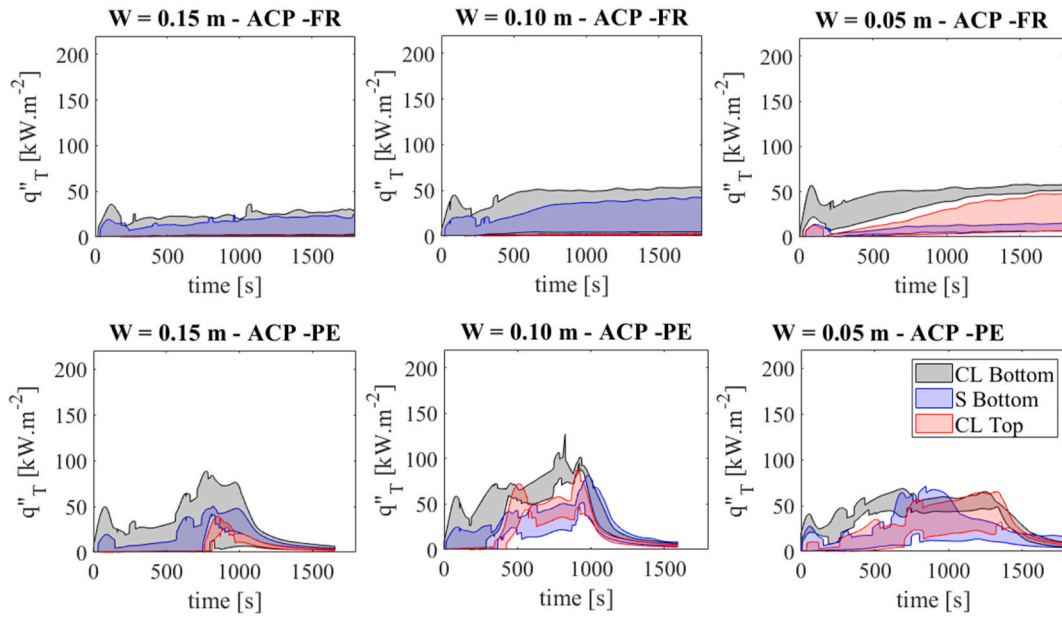


Fig. 8. Flame spread along ACPs.

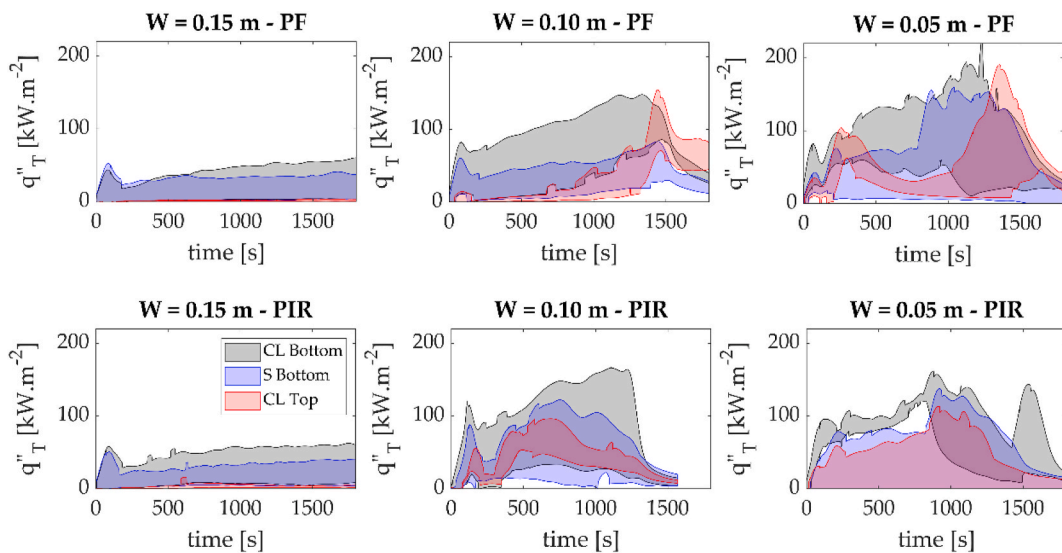


Fig. 9. Flame spread along Insulation foams.

encapsulation layers melted earlier in the test which caused the reduction of the thermal feedback to the opposite wall and allowed for the flame to escape the cavity increasing the heat losses to the environment.

The comparison between these two sets of experiments highlights the impact of the presence of fire-retardant materials which may delay the ignition process and therefore slow or inhibit flame spread; however, whose benefits could be outweighed by the heat transferred in some configurations of system, i.e. if the total external heat flux generated in the cavity surpasses the critical heat flux for ignition and flame spread of one of several components in the assembly. This illustrates the reality that, despite using materials with limited flammability, there are configurations in which the vertical spread of fire is supported by the system, and others where it is not.

The transient profile for the total external heat flux in the systems featuring insulation foams is depicted in Fig. 9. Both insulation foams (PIR and PF) presented a similar fire growth behaviour for the largest cavity width, with limited fire spread through the encapsulation layer. The fire growth was not sustained and it mainly consisted of a flickering fire that was eventually extinguished after a char layer was formed in the insulation core material. It is evident that the raise in the heat flux for all the opposite wall regions is sustained but limited. Considerable fire growth was observed once the cavity width was reduced to 100 mm, reaching the top of the insulation foam. This fire spread can be noticed in total external heat values that surpass  $120 \text{ kW m}^{-2}$ . These high values were measured in a small, localised region and are the result of heat transfer by convection and radiation from the line burner used as source of ignition, and the heat contribution from the combustible material opposite. Garvey et al. showed that the contribution of the heat released by the combustible is the dominating element of the total heat released and transferred in the cavity [36]. Additionally, a typical wall fire with non-combustible linings alone has been measured as  $>120 \text{ kW m}^{-2}$  by Back et al. [37], and with the values obtained in the tests being consistent with previous findings.

Even after flame out was noticed at the bottom centreline regions and smouldering combustion was prevalent at this location, flaming combustion was observed at the top region for the PIR foam for this cavity width. The considerable increase in the heat flux can be attributed to the combustion of a larger area of the insulation foams and the aforementioned increase of the thermal feedback for a reduced cavity width. A faster and more erratic fire spread was observed in both insulation materials for the smallest cavity width. An increase on the external heat flux was also observed for the PF for the 0.05 m cavity when compared to the 0.10 m cavity. This phenomenon can be explained by the previously mentioned factors and by the presence of blocks of hot smouldering foam that landed on the TSCs, increasing the heat transfer by conduction.

The large values for the incident heat fluxes on the opposite wall could have implications on the fire performance of façade assemblies, since they could result in the combustion of other elements, especially for the 0.10 and 0.05 m cavity widths, with external heat fluxes in excess of 120 and  $150 \text{ kW m}^{-2}$  respectively, which result larger than the documented values for critical heat flux for ignition of a number of cladding materials [38] even with the encapsulation not being removed [20]. These findings agree with those in Ref. [19], which found that the ability of the insulation to retain energy within the cavity hence promoting a faster heating of a larger area of the opposing ACP wall, is a factor enhancing the flame spread over the ACM. The presence of these insulation materials combined with a small cavity width could generate flame spread on a system comprised of cladding element initially considered deemed to guarantee no combustion or no fire spread. This highlights how the flammability behaviour of a product might be relevant for the prediction of the fire performance of the system but cannot be used without considering the complex interactions with other design variables in the system.

#### 4. Conclusions

This paper has presented an experimental study to characterise the upward flame spread over four cladding materials: ACP-PE, an aluminium composite panel with a polyethylene core; ACP-FR, an aluminium composite panel with a core comprised of polyethylene and a fire-retardant agent; PF, a phenolic insulation foam; and PIR, a polyurethane-based polyisocyanurate foam. The separation between these linings and a non-combustible wall was also varied with values of 50, 100 and 150 mm. This paper presents the impact of cavity width and material flammability on upward flame spread in a simplified, yet representative setup. By replacing one surface with combustible cladding materials and measuring heat transfer to the non-combustible lining, this paper shows a clearer picture of the influence of these variables in a single-material burning surface scenario, eliminating the confusion of multiple materials burning at once in a typical ventilated façade assembly. The results of this study are a valuable addition to current understanding of the effect of cavity width and material flammability on upward flame spread and pave the way for improved fire safety in façade assemblies.

The thermal behaviour of the materials at bench scale has a relationship to the fire spread in the medium scale setup. The material with the largest HRRPUA in small scale had the larger peak HRR in the intermediate scale, which could also be linked to the fastest ignition and most rapid fire spread among the materials independent of the cavity width.

Encapsulation failure either by melting, cracking or delamination is a critical step for fire spread since it enables the exposure of the flammable core to the heat source and its combustion. It was noticed that once the encapsulation failed the inner core underwent thermal degradation, leading to flame spread when other processes as flame intermittency or charring did not stop the sustained combustion of the material. The failure mechanisms are out of the scope of this research, although they have been characterised to some extent elsewhere [19].

The interaction between the materials in the façade assembly and the cavity could lead to unacceptable fire spread scenarios despite using materials with limited flammability. Screening materials and products is important to identify potential fire spread risk, but a comprehensive analysis at both geometry and system-scale is also needed to uncover further scenarios of unacceptable fire spread.

The paper presents the behaviour for individual materials and might provide the interpretation needed to better understand existing literature which has combustible linings on both sides. However, the interaction between materials with different flammability properties is likely to lead to different results. For example, the presence of high values for the external heat flux on the opposite wall when including a combustible foam might indicate that the contribution of these materials could accelerate the ignition of other cladding materials despite its relatively low HRR when compared with ACP-PE.

The innovative approach presented here, with its experimental setup, enables the comprehensive and systematic characterisation of system behaviour at a representative scale this setup uniquely captures the nuanced and intricate interactions of the system, something that was not possible given more material focused approaches to this problem, or even based on the results of large scale standardised cladding tests such BS8414 or AS5113.

In conclusion, upward flame spread within a cavity is a complex phenomenon that is influenced by a number of factors including the properties of the fuel, the ventilation and geometry of the cavity, and the presence of any fire retardant agents. Future research in this field could focus on understanding the interactions between these factors to better predict and prevent upward flame spread.

#### Author statement

Julian Mendez: Methodology, Formal analysis, Investigation,

Writing - Original Draft, Visualization.

Martyn McLaggan: Conceptualisation, Writing – Review and Editing.

David Lange: Conceptualisation, Writing – Review and Editing.

### Declaration of competing interest

The authors declare that they have no known competing financial interests or personal relationships that could have appeared to influence the work reported in this paper.

### Data availability

Data will be made available on request.

### Acknowledgements

The authors would like to thank Fairview for their generous donation of cladding materials. The manufacturers had no influence on the execution of this work nor the results presented on this research.

### Appendix A. Supplementary data

Supplementary data to this article can be found online at <https://doi.org/10.1016/j.firesaf.2023.104020>.

### References

- [1] E. Antonatus, Facades—fire safety aspects in the context of increasing use of thermal insulation, in: *Interflam 2013: Proceedings of the Thirteenth International Conference*, 2013, pp. 1291–1302.
- [2] L. Peng, Z. Ni, X. Huang, Review on the fire safety of exterior wall claddings in high-rise buildings in China, *Procedia Eng.* 62 (2013) 663–670.
- [3] B. Lane, The Grenfell Tower Inquiry: Dr Barbara Lane's Expert Report (Supplemental). Phase 1 Report- Section 9 Routes for Fire Spread Out through the Window Openings, 2018.
- [4] M.S. McLaggan, et al., Towards a better understanding of fire performance assessment of façade systems: current situation and a proposed new assessment framework, *Construct. Build. Mater.* 300 (Sep. 2021), 124301.
- [5] J.L. Torero, Grenfell Tower Inquiry: Professor Jose Torero Report (Phase 1 - Supplemental), JTOS0000001, 2018.
- [6] A. Sharma, K.B. Mishra, Experimental investigations on the influence of 'chimney-effect' on fire response of rainscreen façades in high-rise buildings, *J. Build. Eng.* 44 (2021), 103257.
- [7] A.C. Fernandez-Pello, T. Hirano, Controlling mechanisms of flame spread, *Combust. Sci. Technol.* 32 (1–4) (1983) 1–31.
- [8] K. Saito, J.G. Quintiere, F.A. Williams, Upward turbulent flame spread, *Fire Saf. Sci.* 1 (1986) 75–86.
- [9] J.G. Quintiere, Fire growth: an overview, *Fire Technol.* 33 (1) (1997) 7–31.
- [10] I.S. Wichman, Theory of opposed-flow flame spread, *Prog. Energy Combust. Sci.* 18 (6) (Jan. 1992) 553–593.
- [11] A.C. Fernandez-Pello, The solid phase, in: G. Cox (Ed.), *Combustion Fundamentals of Fire*, Academic Press, London, 1995.
- [12] H.Y. Shih, H.C. Wu, An experimental study of upward flame spread and interactions over multiple solid fuels, *J. Fire Sci.* 26 (5) (Sep. 2008) 435–453.
- [13] J.E. Mendez, D. Lange, J.P. Hidalgo, M.S. McLaggan, Effect of cavity parameters on the fire dynamics of ventilated façades, *Fire Saf. J.* 133 (October) (2022).
- [14] M. Foley, D.D. Drysdale, Heat transfer from flames between vertical parallel walls, *Fire Saf. J.* 24 (1) (1995) 53–73.
- [15] K. Livkiss, S. Svensson, B. Husted, P. van Hees, Flame heights and heat transfer in façade system ventilation cavities, *Fire Technol.* 54 (3) (2018) 689–713.
- [16] Z. Zhao, F. Tang, L. Chen, J. Zhang, J. Wen, Effect of Parallel Curtain Walls on Upward Flame Spread Characteristics and Mass Loss Rate over PMMA, *Fire Technol.*, 2021.
- [17] W. An, R. Pan, Q. Meng, H. Zhu, Experimental study on downward flame spread characteristics under the influence of parallel curtain wall, *Appl. Therm. Eng.* 128 (2018) 297–305.
- [18] X. Ma, et al., Experimental study of interlayer effect induced by building facade curtain wall on downward flame spread behavior of polyurethane, *Appl. Therm. Eng.* 167 (Feb) (2020).
- [19] L. Bisby, Grenfell Tower Inquiry: Professor Luke Bisby Report (Phase 2 - Experiments Work Package 2- System Interactions), LBYWP200000001, 2021.
- [20] L. Bisby, Grenfell Tower Inquiry: Professor Luke Bisby Report (Phase 2 - Materials Testing Report 1), LBYMT00000002, 2020.
- [21] M.S. McLaggan, et al., Flammability trends for a comprehensive array of cladding materials, *Fire Saf. J.* 120 (May 2020), 103133.
- [22] M.S. McLaggan, et al., The material library for cladding materials in queensland, Australia, in: *3rd International Symposium on Fire Safety of Facades*, 2019.
- [23] M.S. McLaggan, V. Gupta, J.P. Hidalgo, J.L. Torero, Upward flame spread for fire risk classification of high-rise buildings, *Int. J. High-Rise Build.* 10 (4) (Jan. 2021) 299–310.
- [24] J.L.J.L. Torero, Grenfell Tower Inquiry - Phase 2 - Adequacy of the Current Testing Regime, JTOR00000006, 2022.
- [25] A./S. Skamol, V-1100 (375) Vermiculite Insulating Boards - Dataheet, Jul-2012.
- [26] M.S. McLaggan, et al., Protocols for the Material Library of Cladding Materials – Part II: Sample Preparation and Testing Methodologies, 2019. St Lucia, Australia.
- [27] J. Mendez, D. Lange, J.P. Hidalgo, M.S. McLaggan, Experimental study of the fire dynamics in a non-combustible parallel wall setup, in: *Proc. Tenth Int. Semin., Fire Explos. Hazards*, 2022.
- [28] J.P. Hidalgo, C. Maluk, A. Cowlard, C. Abecassis-Empis, M. Krajcovic, J.L. Torero, A Thin Skin Calorimeter (TSC) for quantifying irradiation during large-scale fire testing, *Int. J. Therm. Sci.* 112 (2017) 383–394.
- [29] H. Xu, et al., Large-scale compartment fires to develop a self-extinction design framework for mass timber—Part I: literature review and methodology, *Fire Saf. J.* 128 (2022), 103523.
- [30] J.T. Nakos, Uncertainty Analysis of Thermocouple Measurements Used in Normal and Abnormal Thermal Environment Experiments at Sandia's Radiant Heat Facility and Lurance Canyon Burn Site, 2004. United States.
- [31] E.K. Asimakopoulou, K. Chotzoglou, D.I. Kolaitis, M.A. Founti, Characteristics of externally venting flames and their effect on the façade: a detailed experimental study, *Fire Technol.* 52 (6) (2016) 2043–2069.
- [32] A. Lock, et al., "Experimental Study of the Effects of Fuel Type, Fuel Distribution, and Vent Size on Full-Scale Underventilated Compartment Fires in an ISO 9705 Room (NIST TN 1603)." Technical Note (NIST TN), National Institute of Standards and Technology, Gaithersburg, MD, 2008.
- [33] L. Zhao, N.A. Dembsey, Measurement uncertainty analysis for calorimetry apparatuses, *Fire Mater.* 32 (1) (Jan. 2008) 1–26.
- [34] J.P. Hidalgo, N. Gerasimov, R.M. Hadden, J.L. Torero, S. Welch, Methodology for estimating pyrolysis rates of charring insulation materials using experimental temperature measurements, *J. Build. Eng.* 8 (January) (2016) 249–259.
- [35] M.J. Scudamore, P.J. Briggs, F.H. Prager, Cone calorimetry—a review of tests carried out on plastics for the association of plastic manufacturers in Europe, *Fire Mater.* 15 (2) (1991) 65–84.
- [36] B. Garvey, et al., Experimental methodology to study the fire contribution of cladding materials, *Inter* 15 (2) (2019) 2079–2090.
- [37] G. Back, C. Beyer, P. Dinunno, P. Tatem, Wall incident heat flux distributions resulting from an adjacent fire, *Fire Saf. Sci.* 4 (1994) 241–252.
- [38] M.S. McLaggan, et al., The Material Library of Cladding Materials, Data Collection, The University of Queensland, St Lucia, Australia, 2019.